Spontaneous Deformation of an AdS Spherical Black Hole

Zhuan Ning

School of Physical Sciences, University of Chinese Academy of Sciences

Collaborators: Yu Tian, Qian Chen, Xiaoning Wu, Hongbao Zhang [arXiv:2307.14156]

CCAST 引力/规范对偶及其应用研讨会

December 5, 2023

Outline

Outline

The black hole uniqueness theorem

All stationary, asymptotically flat black holes of the Einstein-Maxwell equations in $d = 4$ dimensions are uniquely specified by their mass, angular momentum, and electric charge, and have horizon topology S^2

Evading the uniqueness theorem:

- different spacetime asymptotics
- additional matter fields
- higher dimensions

In some cases, solutions with additional conserved quantities and other horizon topologies can survive

Black holes in AdS spacetime

- In the background of AdS spacetime, the horizon topology of black holes is not limited to S^2
- Solutions that approach a local AdS spacetime asymptotically can possess a horizon with planar or hyperbolic topology
- These “black holes” have been extensively studied, both analytically and numerically
- In particular, the planar black branes are the main objects of interest due to the AdS/CFT correspondence

Holographic first-order phase transition

Homogeneous planar black hole $\longrightarrow$ inhomogeneous planar black hole

[Attems et al., 2017, Janik et al., 2017]

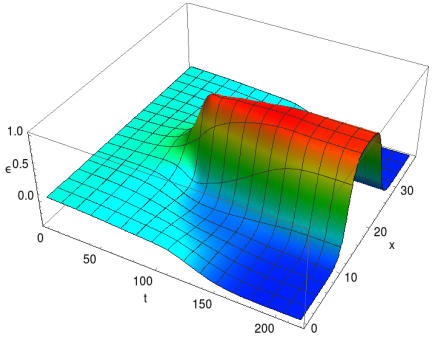

- These configurations do not possess an explicit inhomogeneous external source
- The final state spontaneously breaks translational symmetry
- In the context of holography, this is related to the phase separation process in systems with first-order phase transition

What about spherical black holes?

- Static black hole solutions with either only axial symmetry or no continuous spatial symmetry are constructed in certain models
  [Kichakova et al., 2016, Herdeiro and Radu, 2016, Herdeiro and Radu, 2020]

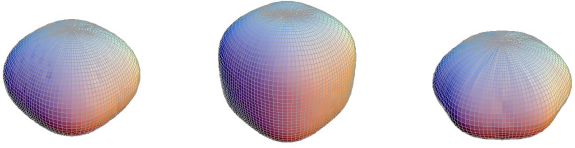

- Are there static black holes with only axial symmetry in the absence of a winding number and a spatially dependent external source?
- Is there a dynamical pathway from a spherically symmetric black hole to a deformed black hole?

Outline

Einstein-scalar model

- The Lagrangian density

$$\mathcal{L} = R - \frac{1}{2}\nabla_\mu\phi\nabla^\mu\phi - V(\phi) \tag{2.1}$$

- We set the AdS radius L to the unit and focus on a scalar field with the mass squared $m^2 = -2$ within the Breitenlohner-Freedman bound. Specifically, the scalar potential is specified as

$$V(\phi) = -6\cosh\left(\frac{\phi}{\sqrt{3}}\right) - \frac{\phi^4}{5} \tag{2.2}$$

- The Einstein equation and the scalar equation

$$\begin{aligned} R_{\mu\nu} - \frac{1}{2}Rg_{\mu\nu} &= \frac{1}{2}\nabla_\mu\phi\nabla_\nu\phi - \left(\frac{1}{4}(\nabla\phi)^2 + \frac{1}{2}V(\phi)\right)g_{\mu\nu} \\ \nabla^\mu\nabla_\mu\phi &= \frac{dV(\phi)}{d\phi} \end{aligned} \tag{2.3}$$

Metric ansatz

- We adopt the ingoing Bondi-Sachs-like coordinates [Cao and He, 2013, He and Cao, 2015] with axial symmetry (all the fields are functions of (v, z, θ)) and no rotation:

$$ds^2 = \frac{L^2}{z^2}(-[fe^{-\chi} - e^A\xi^2]dv^2 - 2e^{-\chi}dvdz - 2\xi e^A dvd\theta + e^A d\theta^2 + e^{-A}\sin^2\theta d\varphi^2) \quad (2.4)$$

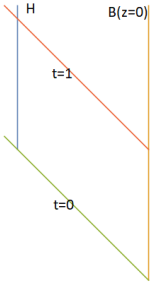

Advantages of numerical relativity under the Bondi-Sachs gauge

- Simplicity of the formalism (to save our brainpower)
- Efficiency of the numerical evolution (to save our computational resources)
- Ability to be used in general complicated systems (collapse/scalarization with less symmetry, AdS/CFT, ...)
- How to illustrate?
  - Black hole dynamics in AdS (this talk)
  - Applied AdS/CFT (superfluid dynamics, holographic solids, AdS/QCD, ...)
  - Black hole dynamics in non-AdS and gravitational waves

Asymptotic behavior of the scalar field

- Near the AdS boundary ($z = 0$), the scalar field has the following asymptotic behavior

$$\phi = \phi_1 z + \phi_2 z^2 + O(z^3) \tag{2.5}$$

- The source ϕ_1 is a boundary freedom
- In the case of planar topology, the scalar source is only a scaling freedom
- But for spherical topology, the different values of the source will result in the physical scenarios with substantial distinctions

Static solutions with spherical symmetry

- ξ and A are turned off, and χ, f, and ϕ are only functions of z
- The equations of motion

$$\chi' = \frac{z}{4}\phi'^2, \tag{2.6}$$

$$\left(\frac{f}{z^3}\right)' = \frac{L^2}{2z^4}e^{-\chi}V(\phi) - \frac{1}{z^2}e^{-A-\chi}, \tag{2.7}$$

$$\frac{z^2}{2}\left(\frac{f\phi'}{z^2}\right)' = \frac{L^2}{2z^2}e^{-\chi}\frac{dV(\phi)}{d\phi}. \tag{2.8}$$

- In the computational domain $[0, z_0]$ of the z coordinate, the boundary conditions

$$\begin{aligned} \chi|_{z=0} &= 0 \\ f|_{z=z_0} &= f_0 \\ \phi'|_{z=0} &= \phi_1 \end{aligned} \tag{2.9}$$

Static solutions with spherical symmetry

- The radial position of the event horizon z_h is determined by the condition

$$f(z_h) = 0 \tag{2.10}$$

- Once the spacetime geometry has been determined, one can easily extract the energy density and the temperature of the gravitational system:

$$\varepsilon = -f_3 + \frac{\phi_1 \phi_2}{6}, \quad T = \frac{|f'(z_h)|}{4\pi} \tag{2.11}$$

where f_3 denotes the coefficient of the cubic term in the asymptotic expansion of the field f near the boundary

Phase diagram

The resulting thermodynamic relation for a scalar source $\phi_1 = 2$

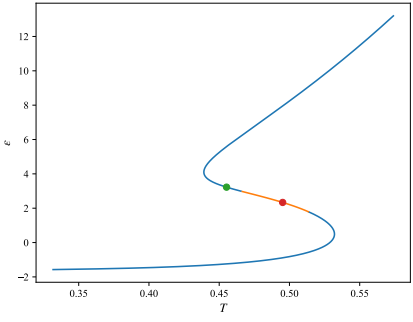

- The spinodal region lies between two turning points
- Due to the negative specific heat, the equilibrium states located in such a spinodal region are thermodynamically unstable
- In the case of planar topology, thermodynamically unstable states are also dynamically unstable
- In the spherical case, this is not necessarily true

Outline

Linear perturbations

- We consider the perturbations on the static, spherically symmetric background

$$\begin{aligned} g_{\mu\nu}(v,z,\theta) &= g^{(0)}_{\mu\nu}(z) + \delta g_{\mu\nu}(v,z,\theta) \\ \phi(v,z,\theta) &= \phi^{(0)}(z) + \delta\phi(v,z,\theta) \end{aligned} \tag{3.1}$$

- To separate the angular dependence, we introduce the new variables

$$\begin{aligned} \delta\Xi &= \frac{1}{\sin\theta}\partial_\theta(\sin\theta\delta\xi) \\ &= \partial_\theta\delta\xi + \cot\theta\delta\xi \\ \delta a &= \frac{1}{\sin\theta}\partial_\theta(\sin\theta(\partial_\theta\delta A + 2\cot\theta\delta A)) \\ &= \partial_\theta^2\delta A + 3\cot\theta\partial_\theta\delta A - 2\delta A \end{aligned} \tag{3.2}$$

- All θ-dependence can be transformed to $\Delta_2 = \frac{1}{\sin\theta}\frac{\partial}{\partial\theta}(\sin\theta\frac{\partial}{\partial\theta})$

Perturbation decomposition

- Since we are only considering the quasi-normal modes with an azimuthal number $m = 0$, we can decompose the perturbations in the following form

$$\delta\Psi = (\delta\chi, \delta\Xi, \delta f, \delta a, \delta\phi) = \tilde{\Psi}(z)e^{-i\omega v}P_l(\cos\theta) \tag{3.3}$$

- Numerical procedure

$$\begin{aligned} \partial_v &\to -i\omega \\ \partial_z &\to \text{Differentiation matrix} \\ \Delta_2 &\to -l(l+1) \end{aligned} \tag{3.4}$$

- Once given a specified angular quantum number l, the quasi-normal frequencies ω can be obtained by solving a generalized eigenvalue problem

Quasi-normal spectra

The region of the states with dynamical instability is marked in orange in the phase diagram

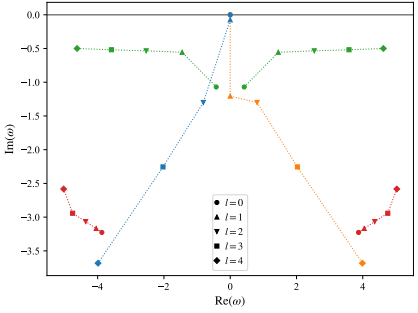

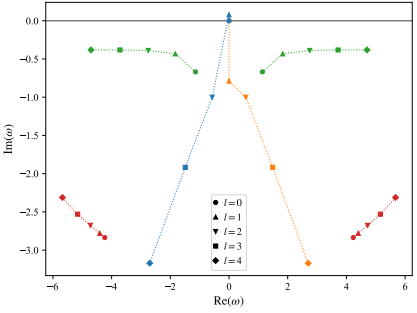

For the state represented by the green dot, all modes lie on or below the real axis, indicating the dynamical stability at the linear level

For the state represented by the red dot, the configuration are dynamically unstable under axial perturbations with $l = 1$

Outline

Axial perturbations

- We introduce a θ-dependent perturbation to the scalar field, the form of which is chosen as a mixture of all modes without loss of generality:

$$\delta\phi(z,\theta) = \phi_0 z^2 \exp\left(-10\sin^2\frac{\theta}{2}\right) \tag{4.1}$$

  where ϕ_0 indicates the amplitude of the perturbation
- For the state represented by the green dot, the amplitude of the perturbation ranges from $\phi_0 = 0.1$ to $\phi_0 = 1$
- For the red dot, the range is $\phi_0 = 0.001$ to $\phi_0 = 0.01$

Nonlinear equations of motion

$$\chi' = \frac{z}{4}(A'^2 + \phi'^2) \tag{4.2}$$

$$\left(\frac{e^{A+\chi}}{z^2}\xi'\right)' = -\frac{1}{z^2}[(A+\chi)'_\theta + \frac{2\chi_\theta}{z} - (A'A_\theta + \phi'\phi_\theta) + 2\cot\theta A'] \tag{4.3}$$

$$\left(\frac{f}{z^3}\right)' = \frac{\xi_\theta}{z^3} + \frac{L^2}{2z^4}e^{-\chi}V(\phi) + \frac{1}{z^2}[P - \cot\theta(Q - \frac{\xi}{z} + \frac{3e^{-A-\chi}A_\theta}{2}) - e^{-A-\chi}] \tag{4.4}$$

$$\dot{A}' - \frac{\dot{A}}{z} = \frac{z^2}{2}\left(\frac{fA' - \xi A_\theta}{z^2}\right)' + \frac{(e^{-A-\chi}A_\theta - \xi A')_\theta}{2} + P + \cot\theta(Q - \frac{\xi A'}{2}) \tag{4.5}$$

$$\dot{\phi}' - \frac{\dot{\phi}}{z} = \frac{z^2}{2}\left(\frac{f\phi' - \xi\phi_\theta}{z^2}\right)' + \frac{(e^{-A-\chi}\phi_\theta - \xi\phi')_\theta}{2} - \frac{L^2}{2z^2}e^{-\chi}\frac{dV(\phi)}{d\phi} \tag{4.6}$$

$$+ \cot\theta(\frac{e^{-A-\chi}\phi_\theta}{2} - \frac{\xi\phi'}{2})$$

Evolution scheme

- Where P and Q are auxiliary variables

$$P = \frac{e^{A+\chi}}{4}\xi'^2 + \frac{\xi_\theta}{z} - \frac{\xi'_\theta}{2} - \frac{e^{-A-\chi}}{4}(2A_\theta\chi_\theta + \chi_\theta^2 - \phi_\theta^2) + \frac{(e^{-A-\chi})_{\theta\theta}}{2}$$
$$Q = \frac{\xi'}{2} - \frac{\xi}{z} + \frac{e^{-A-\chi}\chi_\theta}{2} \tag{4.7}$$

- There is a systematic and efficient integration strategy to solve these equations, which benefits from their nested structure
- Initial time slice: $A, \phi \xrightarrow{(4.2)} \chi \xrightarrow{(4.3)} \xi \xrightarrow{(4.4)} f \xrightarrow{(4.5),(4.6)} \dot{A}, \dot{\phi} \longrightarrow$ next time slice
- Boundary conditions at $z = 0$: energy and momentum conservation of the boundary system

Discretization in the angular direction

- In the θ direction, we extend the coordinate range from $[0, \pi]$ to $[-\pi, \pi]$, such that the periodic boundary condition can be employed with Fourier pseudospectral discretization instead of the traditional Chebyshev one for $\theta \in [0, \pi]$. This method has the following advantages:
  - Avoid dealing with boundary conditions at the north and south poles
  - Greatly improve numerical efficiency and stability in the dynamical evolution
- On the other hand, we utilize an even number of Fourier grid points, denoted as M, ranging from $-\pi + \pi/M$ to $\pi - \pi/M$ to avoid the coordinate singularity at the north and south poles

Apparent horizon

- For axisymmetric configurations, determining the location of the apparent horizon $z = h(v, \theta)$ requires the following condition

$$(\partial_\theta + h_\theta \partial_z)(\xi + h_\theta e^{-A-\chi}) + \cot\theta(\xi + h_\theta e^{-A-\chi}) = -\frac{1}{h}(f - h_\theta^2 e^{-A-\chi}) \tag{4.8}$$

  where all fields (except h and its θ-derivative) should be understood as functions of v, $z = h(v, \theta)$, and θ

- It is convenient to define the average entropy density as follows

$$\bar{s} = \frac{\int_0^\pi s(\theta) \sin\theta d\theta}{\int_0^\pi \sin\theta d\theta} = \int_0^\pi \frac{\pi}{h^2} \sin\theta d\theta \tag{4.9}$$

Time evolution for the stable state

Temporal and spatial dependence of the apparent horizon configuration for the initial state represented by the green dot

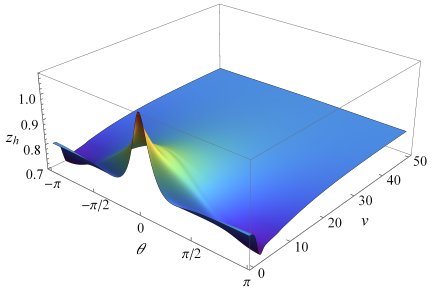

- Our numeric simulations demonstrate that the axial perturbation damps over time, leaving a spherically symmetric black hole
- Confirming the dynamical stability, consistent with the linear analysis

Time evolution for the unstable state

Angular dependence of the apparent horizon configurations z_h at different times for the initial state represented by the red dot

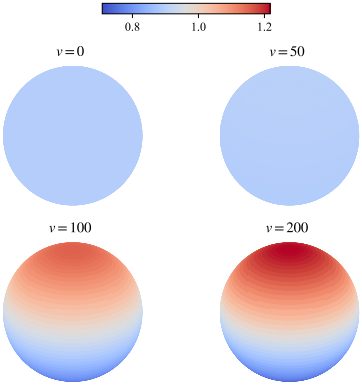

- The unstable mode with angular quantum number $l = 1$ is excited under the axial perturbation, leading to drastic changes in the gravitational configuration
- The apparent horizon radius $r_h = z_h^{-1}$ decreases at the north pole region and increases at the south pole region, eventually leading to the formation of a black hole with only axial symmetry

Time evolution for the unstable state

Angular dependence of the final horizon configuration

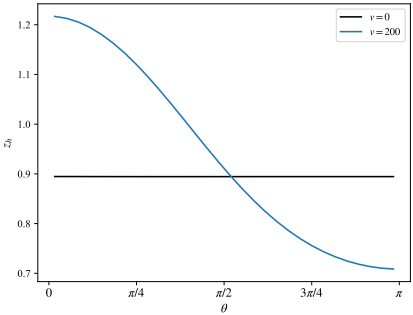

- A strong θ-dependence in the final state while the scalar source remains isotropic throughout the time evolution
- Therefore, the spherical symmetry of the gravitational system is broken spontaneously, resulting in a dynamical deformation process

The second law of black hole mechanics

Temporal evolution of the average entropy density for the initial state represented by the red dot

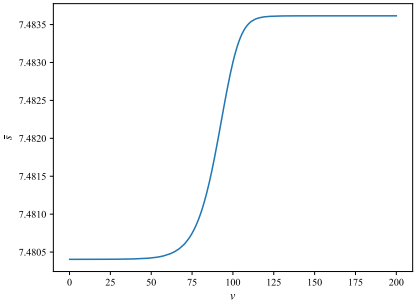

- The second law of black hole mechanics asserts that black hole entropy never decreases during evolution
- Although the apparent horizon exhibits distinct dynamical behavior in different angular regions, its total area always increases monotonically with time
- Confirming the satisfaction of the second law of black hole mechanics in our cases

Outline

Summary

- Applying numerical relativity under the Bondi-Sachs gauge to an AdS spherical black hole with a scalar field, we achieve:
  - A spinodal region is discovered in the phase diagram for static solutions with spherical symmetry
  - We identify unstable quasi-normal modes for certain non-zero angular quantum numbers in some states located in the spinodal region
  - Axial scalar perturbations in nonliear dynamical evolution lead to the emergence of deformed black holes, which spontaneously break spherical symmetry

Outlook

- Implications related to AdS/CFT?
- How to extend to rotating black holes?

$$(h_{ij}) = \begin{pmatrix} e^{A}\cosh B & \sinh B \sin\theta \\ \sinh B \sin\theta & e^{-A}\cosh B \sin^2\theta \end{pmatrix} \tag{5.1}$$

- How to extend to other asymptotics than AdS?

Thank You!


Attems, M., Bea, Y., Casalderrey-Solana, J., Mateos, D., Triana, M., and Zilhao, M. (2017).
Phase Transitions, Inhomogeneous Horizons and Second-Order Hydrodynamics.
JHEP, 06:129.


Cao, Z. and He, X. (2013).
Generalized Bondi-Sachs equations for characteristic formalism of numerical relativity.
Phys. Rev. D, 88(10):104002.


He, X. and Cao, Z. (2015).
New Bondi-type outgoing boundary condition for the Einstein equations with cosmological constant.
Int. J. Mod. Phys. D, 24(10):1550081.


Herdeiro, C. and Radu, E. (2020).
Static black holes without spatial isometries: from AdS multipoles to electrovacuum scalarization.
Int. J. Mod. Phys. D, 29(11):2041016.


Herdeiro, C. A. R. and Radu, E. (2016).
Static Einstein-Maxwell black holes with no spatial isometries in AdS space.
Phys. Rev. Lett., 117(22):221102.


Janik, R. A., Jankowski, J., and Soltanpanahi, H. (2017).
Real-Time dynamics and phase separation in a holographic first order phase transition.
Phys. Rev. Lett., 119(26):261601.


Kichakova, O., Kunz, J., Radu, E., and Shnir, Y. (2016).
Static black holes with axial symmetry in asymptotically AdS_4 spacetime.
Phys. Rev. D, 93(4):044037.